*Int. J. Solids Structures* Vol 20, No. 2, pp. 167–178, 1984
Printed in Great Britain.

0020-7683/84 $3.00 + .00


# A UNIFIED SOLUTION FOR VARIOUS BOUNDARY CONDITIONS FOR THE COUPLED FLEXURAL–TORSIONAL INSTABILITY OF CLOSED THIN-WALLED BEAM-COLUMNS

ASHOK JOSHI and S. SURYANARAYAN
Department of Aeronautical Engineering, Indian Institute of Technology, Bombay, India

(*Received* 27 *December* 1982)

**Abstract**—The problem of coupled flexural–torsional instability of closed thin-walled beam-columns under the combined action of axial loads and equal end moments is studied numerically. The characteristic equations for stability are obtained and the load interaction curves and mode shapes are plotted for various boundary conditions. From a study of the numerical results and the characteristic equations, equivalent load and geometry parameters are defined. These yield a single solution common for all boundary conditions for the load interaction curve and the mode shape. The effect of various boundary conditions and mode numbers is manifest only in the value of an eigen coefficient independent of the loads which is used in defining the equivalent parameters. The case of lateral instability within the elastic limit is also examined and it is shown that even when tensile axial loads are present elastic lateral instability may occur.

## NOTATION

| | |
|---|---|
| $A$ | area of the cross-section of beam |
| $A_1, A_2, B_1, B_2$ | |
| $C_1, C_2, D_1, D_2$ | arbitrary constants in eqn (9) |
| $D$ | differential operator, $d/d\bar{z}$ |
| $b$ | width of the cross-section |
| $\bar{b}$ | $b/d$, size ratio of the cross-section |
| $d$ | depth of the cross-section |
| $E$ | Young's modulus of elasticity |
| $f$ | $(= \bar{M}\sqrt{(S)}/\bar{P} + S)$, eqn (10) |
| $G$ | shear modulus of rigidity |
| $I_{xx}$ | moment of inertia about x-axis |
| $I_{yy}$ | moment of inertia about y-axis |
| $I_p$ | polar moment of inertia |
| $J$ | St. Venant torsional constant |
| $L$ | span of beam |
| $L_e$ | $(= L/\alpha)$, effective span of beam |
| $M_{yy}$ | moment about y-axis |
| $\bar{M}$ | dimensionless moment defined by eqn (2) |
| $\bar{M}_e$ | $(= \bar{M}/\alpha)$, effective moment parameter |
| $\bar{M}_e^*$ | equivalent moment parameter defined by eqn (24) |
| $M_{cr}$ | critical lateral instability moment for simply-supported ends (eqn 2) |
| $m$ | mode number |
| $P$ | axial load |
| $P_{cr}$ | critical Euler buckling load for simply-supported ends (eqn 2) |
| $\bar{P}$ | $(P/P_{cr})$, dimensionless load parameter |
| $\bar{P}_e$ | $(\bar{P}/\alpha^2)$, effective load parameter |
| $S$ | slenderness parameter defined by eqn (5a) |
| $S_e$ | $(S/\alpha^2)$, effective slenderness parameter |
| $t$ | thickness of the wall of the beam |
| $v_0$ | flexural displacement in y-direction |
| $\bar{v}_0$ | $(v_0(I_p/A)^{-1/2})$, dimensionless displacement |
| $x, y, z$ | Cartesian coordinates, see Fig. 1 |
| $\bar{z}$ | $(= z/L)$, dimensinless spanwise coordinate |
| $\alpha$ | eigen value coefficient |
| $\eta$ | $(= -\bar{v}_0/\theta)$, location of centre of rotation of the cross-section |
| $\eta_e$ | defined by eqns (20) and (23) |
| $\eta_e^*$ | defined by eqn (25) |
| $\epsilon_{limit}$ | linear elastic limit strain |
| $\sigma_{zz}$ | axial stress |
| $\theta$ | torsional displacement |

## 1. INTRODUCTION

The problem of coupled flexural–torsional instability of beam-columns (also referred to in literature as lateral instability) under the combined action of axial load and end moment has

been a subject of study for nearly half a century. The earlierst comprehensive review on "The Lateral Buckling of Beams" is that of Timoshenko[1]. Since then numerous studies considering various types of loads, geometries and end conditions have appeared in the literature. Johnston[2] has studied the eccentrically loaded $I$-column for lateral instability for two cases of simply supported and clamped ends. He has also given the limiting values of the slenderness of the beam for which elastic lateral instability precedes yielding. Goodier[3] has considered singly-symmetric open section beams but restricted to simply-supported end conditions. Salvadori[4] has considered the lateral instability of beams subjected to unequal end moments and axial thrust and by using the concept of an effective span obtained a single interaction equation for simply-supported as well as clamped ends. Many other investigators[5–7] have tackled the problem of lateral instability for various problem parameters like biaxial moment, boundary conditions etc. However their studies usually give separate solutions for different cases as represented by the boundary condition, slenderness of the beam and combination of loads. Only for the simple case of Euler buckling of beams, a completely unified solution for various homogeneous boundary conditions has been obtained using the concept of "effective wave length". That such a unification is possible to account for various homogeneous boundary conditions and slenderness of the beam even for the case of coupled flexural–torsional instability of closed thin-walled beams under the combined action of axial loads and moment constant along the span does not seem to have been realized. The authors have shown in an earlier work[8] that a unified solution can be obtained for various slendernesses of the beam for the coupled flexural–torsional vibration and stability of simply-supported narrow rectangular beams. The present paper gives a unified solution for various boundary conditions for the coupled flexural–torsional instability of closed thin-walled beams subjected to the combined action of axial load and moment constant over the span. It is assumed that the effect of axial constraint stresses arising from the torsion of the cross-section can be ignored. The analysis is also applicable to open cross-sections for which this assumption is valid and is exact for warpless cross-sections, i.e. sections which do not warp under torsion.

Firstly, solutions are obtained for various homogeneous boundary conditions. From an observation of these solutions and the values of the eigen coefficients which represent the effect of various boundary conditions and mode numbers, the various dimensionless load and geometry parameters are redefined to yield a nearly unified solution for the load interaction curve and the mode shape. Further, by incorporating the effect of the slenderness of the stream into the definition of the equivalent moment and the mode shape parameters, the solution is so obtained that (i) the load interaction curve and the mode shape in terms of the equivalent load parameters is independent of the boundary conditions, mode numbers and the slenderness of the beam and (ii) the characteristic equation for the eigen coefficients is entirely in terms of the boundary conditions and mode numbers and independent of the applied loads and the slenderness of the beam. The load interaction equation in terms of equivalent axial loads and moment parameters is similar to the one for simply-supported ends already obtained in literature. The characteristic equations for the eigen coefficient are the same as those obtained for the Euler buckling of columns.

Further to the unified solution, the extent of validity of linear stability analysis as given by the unified solution is also examined for typical geometries of closed and open warpless cross-sections. This is done by dividing the load and geometry planes into elastic and inelastic domains by constant limit strain curves. From these the combinations of load and geometry parameters for which the linear elastic analysis is valid are obtained.

## 2. FORMULATION AND SOLUTION

Figure 1 shows a uniform beam of warpless cross section subjected to an axial load "$P$" and an end Momemt "$M_{yy}$". The governing equations for the coupled flexural ($y$) and torsional ($\theta$) motion of the beam are,

$$\begin{aligned} -EI_{xx}\frac{d^4v_0}{dz^4} + P\frac{d^2v_0}{dz^2} + M_{yy}\frac{d^2\theta}{dz^2} = 0 \\ \left(GJ + \frac{PI_p}{A}\right)\frac{d^2\theta}{dz^2} + M_{yy}\frac{d^2v_0}{dz^2} = 0 \end{aligned} \tag{1}$$

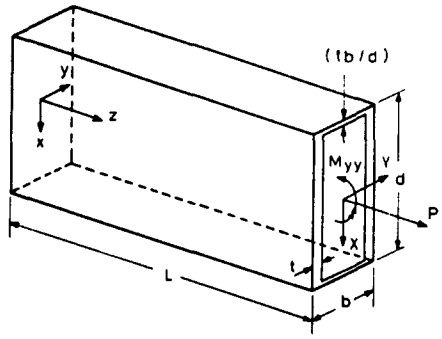


Fig. 1. A typical thin-walled beam of warpless cross-section.

where $A$ is the area of cross-section; $I_{xx}$, $I_{yy}$ are the second moments of area about $x$ and $y$ axes respectively; $I_p$ is the polar moment of inertia, $J$ is the torsional constant; $E$ and $G$ are material constants and $v_0$ and $\theta$ are the infinitesimal flexural (y) and torsional displacements of the cross-section. Using the following transformations

$$z = \bar{z}L, \quad P = \bar{P}P_{cr}, \quad M_{yy} = \bar{M}M_{cr}$$

where

$$P_{cr} = \frac{\pi^2 EI_{xx}}{L^2}, \quad M_{cr} = \frac{\pi}{L}\sqrt{(EI_{xx}GJ)} \tag{2}$$

we get the governing equations as

$$-\frac{EI_{xx}}{L^4}\frac{d^4v_0}{d\bar{z}^4} + \frac{\bar{P}\pi^2 EI_{xx}}{L^4}\frac{d^2v_0}{d\bar{z}^2} + \bar{M}\frac{\pi}{L^3}\sqrt{(EI_{xx}GJ)}\frac{d^2\theta}{d\bar{z}^2} = 0$$

$$\left(\frac{GJ}{L^2} + \frac{\bar{P}\pi^2 EI_{xx}I_p}{AL^4}\right)\frac{d^2\theta}{d\bar{z}^2} + \bar{M}\frac{\pi}{L^3}\sqrt{(EI_{xx}GJ)}\frac{d^2v_0}{d\bar{z}^2} = 0. \tag{3}$$

Simplification of eqns (3) yields

$$-\frac{d^4v_0}{d\bar{z}^4} + \pi^2\bar{P}\frac{d^2v_0}{d\bar{z}^2} + \bar{M}\pi L\sqrt{\left(\frac{GJ}{EI_{xx}}\right)}\frac{d^2\theta}{d\bar{z}^2} = 0$$

$$\frac{\bar{M}\pi LA}{I_p}\sqrt{\left(\frac{GJ}{EI_{xx}}\right)}\frac{d^2v_0}{d\bar{z}^2} + \left(\frac{GJAL^2}{EI_{xx}I_p} + \pi^2\bar{P}\right)\frac{d^2\theta}{d\bar{z}^2} = 0. \tag{4}$$

Defining a slenderness parameter $S$ as

$$S = GJAL^2/(\pi^2 EI_{xx}I_p) \tag{5a}$$

and the dimensionless transverse displacement as

$$\bar{v}_0 = v_0(I_p/A)^{-1/2} \tag{5b}$$

and substituting into the eqn (4) we get

$$\begin{bmatrix} -\frac{1}{\pi^2}D^4 + \bar{P}D^2 & \bar{M}\sqrt{(S)}D^2 \\ \bar{M}\sqrt{(S)}D^2 & (\bar{P}+S)D^2 \end{bmatrix}\begin{Bmatrix} \bar{v}_0 \\ \theta \end{Bmatrix} = 0 \tag{6}$$

where $D$ is the differential operator $d/d\bar{z}$.

From eqn (6) we get

$$D^2(D^2 + \pi^2\alpha^2)\bar{v}_0, \theta = 0 \tag{7}$$

where

$$\alpha^2 = \frac{\bar{M}^2 S}{\bar{P} + S)} - \bar{P}. \tag{8}$$

The general solution for $\bar{v}_0$ and $\theta$ can be expressed as;

$$\begin{aligned} \bar{v}_0(\bar{z}) &= A_1 + B_1\bar{z} + C_1 \sin \alpha\pi\bar{z} + D_1 \cos \alpha\pi\bar{z} \\ \theta(\bar{z}) &= A_2 + B_2\bar{z} + C_2 \sin \alpha\pi\bar{z} + D_2 \cos \alpha\pi\bar{z}. \end{aligned} \tag{9}$$

The above general solution contains 8 arbitrary constants of which only six are independent. By substituting the general solution (9) in one of the eqn (6) we get

$$C_2 = fC_1, \quad D_2 = fD_1, \quad \text{where } f = \frac{\bar{M}\sqrt{(S)}}{\bar{P} + S}. \tag{10}$$

Substituting this into eqn (9) we get the general solution as;

$$\begin{aligned} \bar{v}_0(\bar{z}) &= A_1 + B_1\bar{z} + C_1 \sin \pi\alpha\bar{z} + D_1 \cos \pi\alpha\bar{z} \\ \theta(\bar{z}) &= A_2 + B_2\bar{z} + fC_1 \sin \pi\alpha\bar{z} + fD_1 \cos \pi\alpha\bar{z}. \end{aligned} \tag{11}$$

When various types of boundary conditions are applied to (11), various transcendental characteristic equations are obtained from which the values of the eigen coefficient $\alpha$ can be obtained. With appropriate values assigned to $\alpha$ eqn (8) can itself be considered to represent the stability equation or the load interaction curve. Now let us consider the solution for various classical homogeneous boundary conditions.

(i) *Pinned–pinned ends.* The characteristic equation for this case is

$$\text{Sin } \pi\alpha\bar{z} = 0; \quad \pi\alpha = m\pi \quad \text{or } \alpha = m \tag{12a}$$

and the corresponding normalized mode shape is

$$\bar{v}_0 = \sin \alpha\pi\bar{z}, \quad \theta = f \sin \alpha\pi\bar{z} \tag{12b}$$

(ii) *Clamped–clamped ends.* The characteristic equation is

$$2 \cos \pi\alpha\bar{z} + \pi\alpha \sin \pi\alpha\bar{z} - 2 = 0, \tag{13a}$$

and the mode shape is

$$\bar{v}_0 = 1 - \cos \pi\alpha\bar{z}, \quad \theta = f\bar{v}_0. \tag{13b}$$

(iii) *Clamped–free ends.* The characteristic equation is

$$\text{Cos } \pi\alpha = 0; \quad \pi\alpha = (m - 1/2)\pi \quad \text{or } \alpha = m - 1/2 \tag{14a}$$

and the mode shape is

$$\bar{v}_0 = 1 - \cos \pi\alpha\bar{z}, \quad \theta = f\bar{v}_0. \tag{14b}$$

(iv) *Clamped–pinned ends.* The characteristic equation is

$$\pi\alpha = \tan \pi\alpha \tag{15a}$$

and the mode shape is

$$\bar{v}_0 = \sin \pi\alpha\bar{z} - \pi\alpha\bar{z} - \pi\alpha\,(\cos \pi\alpha\bar{z} - 1);\ \theta = f\bar{v}_0. \tag{15b}$$

(v) *Pinned–free ends.* The first mode for this case represents the rigid body rotation of the beam and for higher modes the characteristic equation for $\alpha$ and normalized mode are respectively,

$$\sin \pi\alpha = 0;\quad \alpha = m \tag{16a}$$

and

$$\bar{v}_0 = \sin \pi\alpha\bar{z};\quad \theta = f\bar{v}_0. \tag{16b}$$

The second mode for this case is the same as the first mode for pinned–pinned ends.

(vi) *Free–free ends.* For this case also the first mode is the rigid body motion of the beam and higher modes are given by eqns (16a) and (16b).

## 3. RESULTS FOR VARIOUS BOUNDARY CONDITIONS

Table 1 gives the values of the eigen coefficient $\alpha$ for various boundary conditions and mode numbers. Figure 2 shows the load interaction curves for various boundary conditions for an infinitely slender beam and a very short beam of $d/L = 0.25$. Though the analysis here is restricted to only Euler–Bernoulli beams, to show the limited extent of the effect of $d/L$ on the results an extreme value of 0.25 is chosen. Curves marked ② correspond to the first mode for simply-supported ends and the second mode for both simply-supported free and free–free ends. Figure 3 shows the spanwise distribution of lateral displacements $\bar{v}_0$ and torsional displacement $\theta$. It can be seen that both have the same spanwise distribution which is independent of the applied loads. However $\eta(= -\bar{v}_0/\theta)$ which gives the location of the centre of rotation of the cross-section, does depend on the applied loads as shown in Fig. 4. The variation of $\eta$ with $\bar{M}$ is shown for two boundary conditions and two typical values of the slenderness. These show that for $d/L = 0.25$ the effect of boundary condition on the value of $\eta$ is noticeable but as the beam becomes slender ($d/L = 0.1$) this effect diminishes.

## 4. DERIVATION OF THE UNIFIED SOLUTION

The load interaction curves in Fig. 2 and the eqn (8) suggest that it is possible to collapse them into a single curve. By defining equivalent axial load, and moment and slenderness parameters $\bar{P}_e$, $\bar{M}_e$ and $S_e$, using the following transformation relations;

$$\bar{M}_e = \bar{M}/\alpha,\quad \bar{P}_e = \bar{P}/\alpha^2 \quad \text{and } S_e = S/\alpha^2 \tag{17}$$

Table 1. Values of the coefficient $\alpha$ for various boundary conditions and mode numbers

| Boundary Condition | Mode Number 1 | 2 | 3 | 4 |
|---|---|---|---|---|
| pinned–pinned | 1.0000 | 2.0000 | 3.0000 | 4.0000 |
| pinned–free | 0.0000 | 1.0000 | 2.0000 | 3.0000 |
| free–free | 0.0000 | 1.0000 | 2.0000 | 3.0000 |
| clamped–pinned | 1.4303 | 2.4590 | 3.4709 | 4.4774 |
| clamped–clamped | 2.0000 | 2.8606 | 4.0000 | 4.9180 |
| clamped–free | 0.5000 | 1.5000 | 2.5000 | 3.5000 |

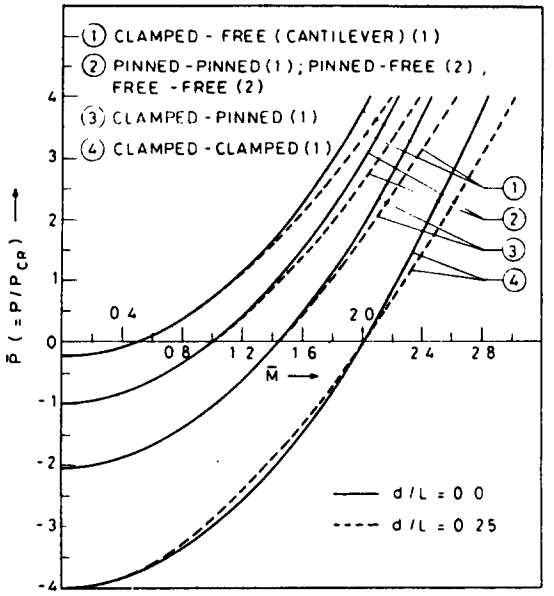


Fig. 2. Interaction curves for various end conditions and two typical values of the slenderness.

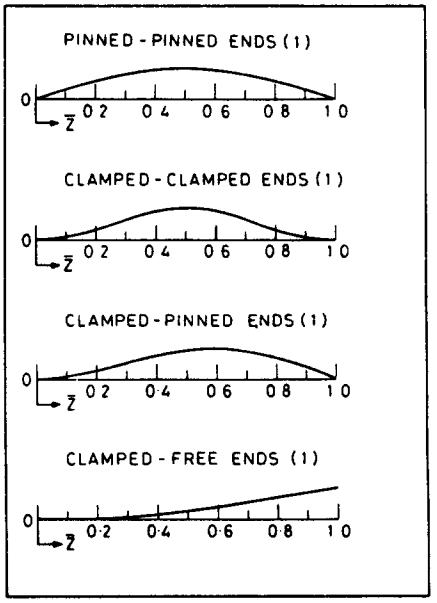


Fig. 3. Normalized spanwise distribution of displacements $\bar{v}_0$ and $\theta$.

and substituting in eqn (8), the interaction equation may be rewritten as,

$$\frac{\bar{M}_e^2}{1+\bar{P}_e/S_e} - \bar{P}_e = 1. \tag{18}$$

Figure 5 shows the above relation for three typical values of the effective slenderness of the beam. It can be seen that for slender beam the interaction equation (18) reduces to

$$\bar{M}_e^2 - \bar{P}_e \approx 1 \tag{19}$$

and that for $d/L_e = 0.1$ where $L_e = L/\alpha$ the deviation in $\bar{M}_e$ even for large tensile axial load

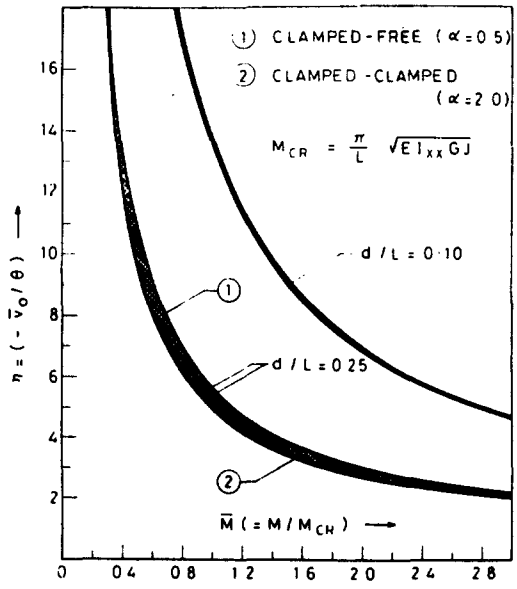


Fig. 4. Location of centre of rotation of the cross-section for various values of $\alpha$ and slenderness of the beam.

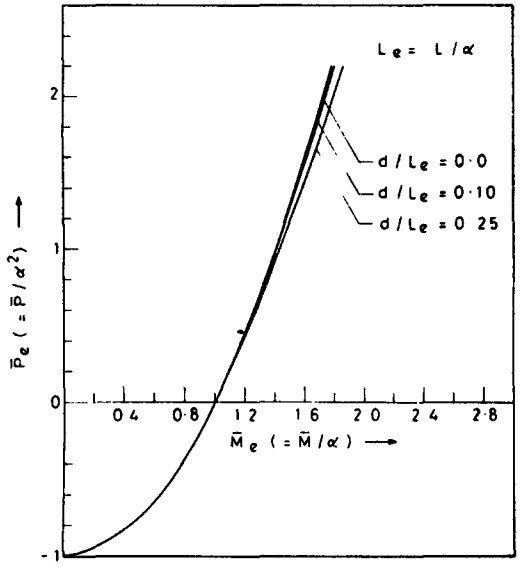


Fig. 5. Nearly unified stability solution showing the effect of effective slenderness.

($\bar{P}_e = 2$) is only about 0.7%. The location of the centre of rotation of the cross-section which represents the coupled mode shape can also be given in terms of an equivalent parameter $\eta_e$ as

$$\eta_e = \eta/\sqrt{(S_e)} = \frac{1 + \bar{P}_e/S_e}{\bar{M}_e} \tag{20}$$

which for a slender beam can be written as,

$$\eta_e \approx 1/\bar{M}_e \tag{21}$$

Figure 6 shows the variation of $\eta_e$ with $\bar{M}_e$ for three typical values of the slenderness and it can be seen that for $d/L_e = 0.1$ the effect of slenderness is only marginal. Results of Figs. 5 and 6 show that for all practical purposes eqns (19) and (21) represent a unified solution. However if it

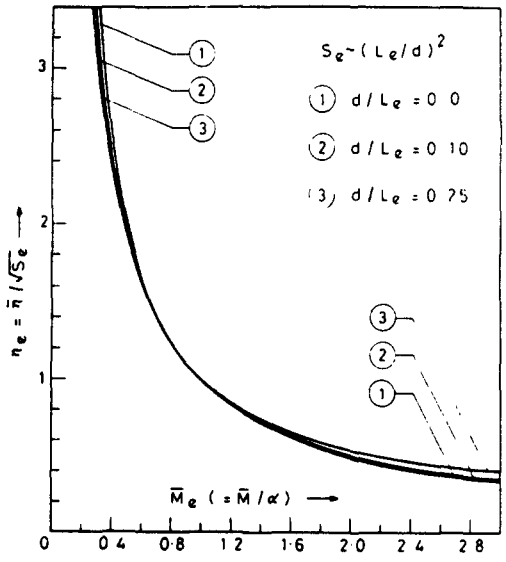


Fig. 6. Nearly unified mode shape showing the effect of effective slenderness.

is desired a completely unified solution accounting for the effect of finite slenderness can also be arrived at as given by

$$\bar{M}_e^{*2} = \bar{P}_e = 1 \tag{22}$$

$$\eta_e^* = 1/\bar{M}_e^*. \tag{23}$$

It can be seen that the load interaction curve is a parabola and the variation of the centre of rotation with the applied moment a hyperbola (see Fig. 7). The parameters $\bar{M}_e^*$ and $\eta_e^*$ can be obtained from eqns (18), (20), (22) and (23) as solutions of the following equations.

$$\bar{M}_e^{*4}/S_e + \bar{M}_e^{*2}(1 - 1/S_e) = \bar{M}_e^2 \tag{24}$$

$$\eta_e^* = \eta_e/\sqrt{(1 + (\bar{M}_e^{*2} - 1)/S_e)}. \tag{25}$$

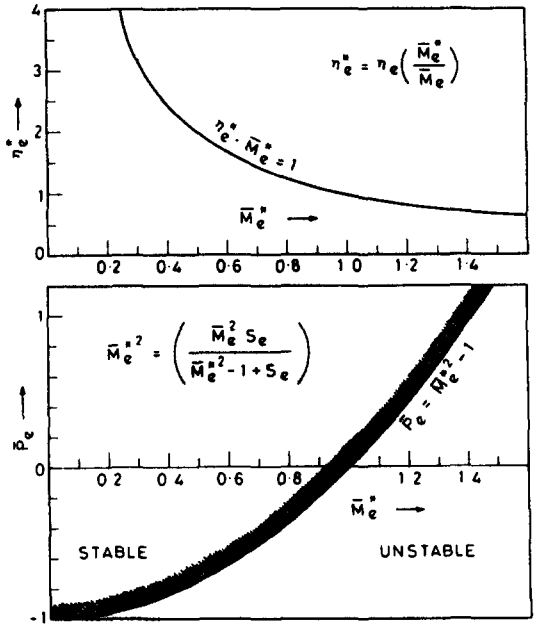


Fig. 7. Unified linear stability solution.

Figures 8 and 9 show the variations of $\bar{M}_e^*$ and $\eta_e^*$ with $\bar{M}_e$. It can be seen that $\bar{M}_e^* \to \bar{M}_e$ and $\eta_e^* \to \eta_e$ as $d/L_e \to 0$. For finite values of $d/L_e$, $\bar{M}_e^*$ differs from $\bar{M}_e$ and $\eta_e^*$ from $\eta_e$ by only a small amount which is of the order of 1/2–1%.

Thus a unified solution for the coupled flexural–torsional instability for all boundary conditions, mode numbers, slenderness of the beam and the load ratio is obtained. This is in such a form that the (i) load interaction curve is independent of the boundary condition and mode number and (ii) the characteristic equation for the eigen coefficient $\alpha$ is independent of the loads. Further it may be observed that (i) the load interaction equation in terms of $\bar{M}_e^*$ and $\bar{P}_e$ is similar to that obtained for the case of simply-supported ends and (ii) the characteristic equations for $\alpha$ are the same as those for the simple case of Euler Buckling.

## 5. LIMITS OF ELASTIC ANALYSIS

The load interaction curves show that the lateral instability is possible even when tensile axial loads are present. The assumption of linear elasticity have been implicit in the present formulation and therefore the interaction curves necessarily represent the linear elastic instability. It would be relevant to examine whether linear elastic instability is at all possible when tensile axial loads are present and if so what are the limits on the loads and the geometries. This

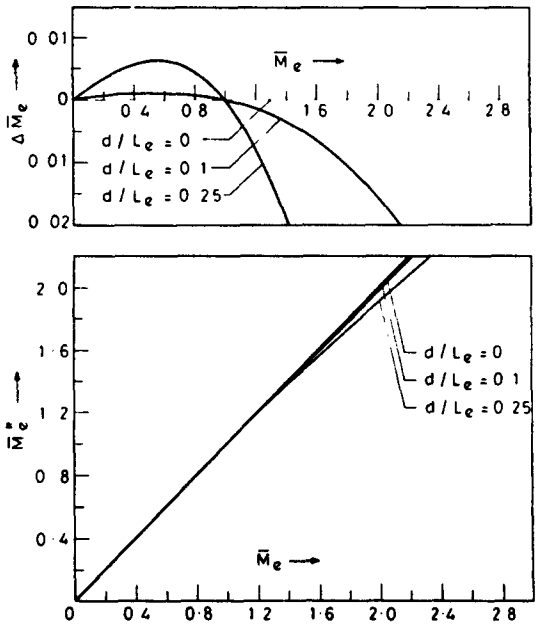


Fig. 8. Equivalent moment $\bar{M}_e^*$ and correction $\Delta\bar{M}_e$ for various values of slenderness.

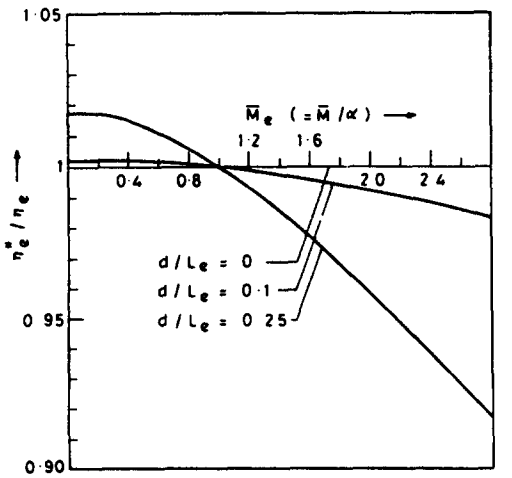


Fig. 9. Correction for unified mode shape for typical values of effective slenderness of the beam.

has been done for the thin-walled beams of typical cross-sections considering various combinations of load and geometry parameters and calculating the maximum strain attained. Figure 10 shows the constant limit strain curves for a simply-supported narrow rectangular beam for some typical combinations of instability load. The straightline corresponds to the case of Euler buckling. The curve corresponding to lateral instability under pure moments is a parabola. Limit strain curves for two typical cases of lateral instability under the tensile axial loads are also plotted. These constant limit strain lines divide the geometry plane defined by $(L_e/d)$ and $(t/d)$ into the elastic zone and inelastic zone. Results show that for a limit strain equal to 0.001 the Euler buckling is elastic for $L_e/t$ values above 30. Elastic lateral instability under pure moments is possible for $(L_e/d)$ value greater than 20 for $t/d = 0.1$ and greater than 80 for $t/d = 0.2$. Similarly elastic lateral instability under tensile axial load ($\bar{P}_e = 0.5$) is possible for $(L_e/d)$ value greater than 25 for $t/d = 0.1$ and greater than 55 for $t/d = 0.15$. It is clear from these results that elastic lateral instability is possible for practically realizable geometries even in the presence of tensile axial loads. In Fig. 11 the limit strain curves for simply supported narrow rectangular

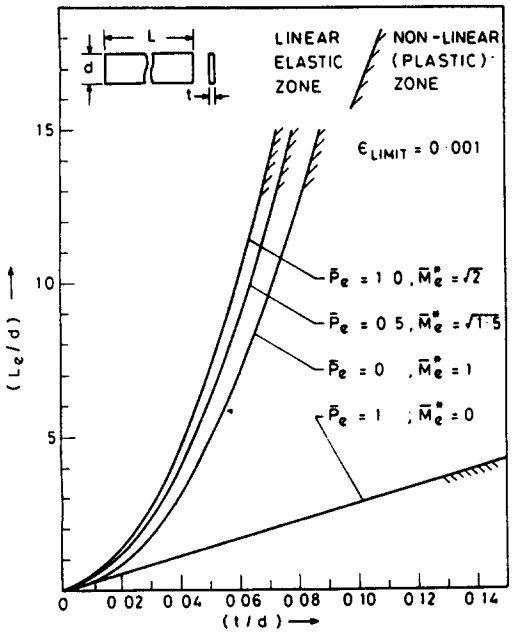


Fig. 10. Constant limit strain curves for simply-supported narrow rectangular beam for various load combinations.

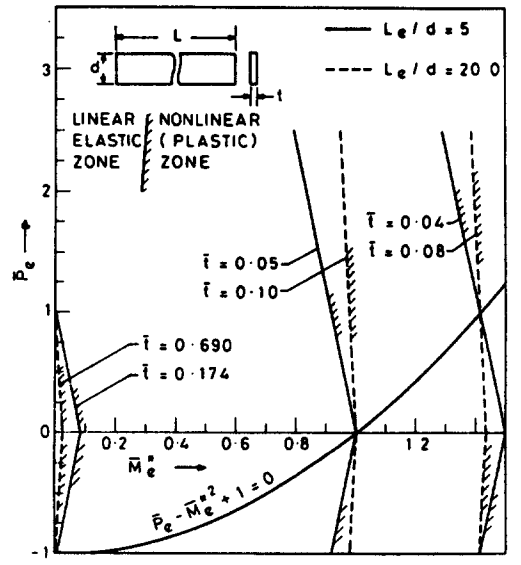


Fig. 11. Constant limit strain curves superimposed on the unified stability solution in load plane.

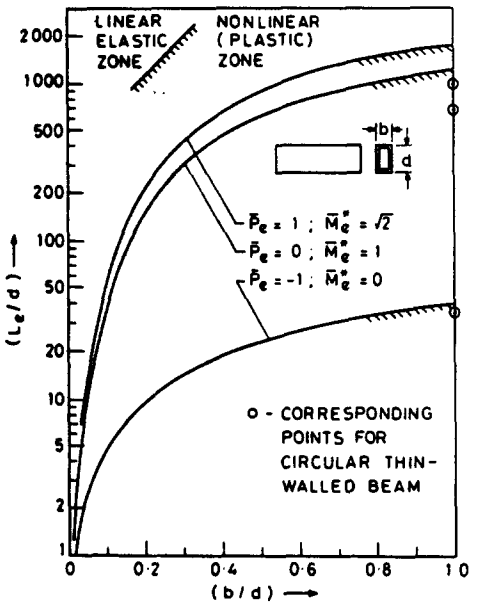


Fig. 12. Constant limit strain curves for a simply-supported warpless rectangular box beam for various load combinations.

beam are superimposed on the unified stability solution in the load plane for two typical values of the slenderness of the beam. These show that the constant strain lines are straight in the load plane and are near vertical for $L_e/d = 20$. Figure 12 shows the constant limit strain curves on a semi-log scale for a simply-supported warpless rectangular box section. The results show that elastic lateral instability is possible even for closed sections of sufficiently deep geometries. For $(b/d)$ value of 0.1 elastic lateral instability under pure moments is possible for $(L_e/d)$ value greater than 40. The value of $(L_e/d)$ for elastic lateral instability under tensile axial load ($\bar{P}_e = 1$) for $(b/d)$ value of 0.1 is 57. However for higher values of $(b/d)$ this limiting value of $(L_e/d)$ increases sharply. For $(b/d) = 0.25$ the corresponding values of $(L_e/d)$ are 215 and 320 and for $(b/d) = 0.5$ the corresponding values are 620 and 880. For $b/d = 1.0$ (square box) elastic lateral instability under pure moments is possible for $(L_e/d)$ value greater than 1200. The corresponding value for $\bar{P}_e = 1$ is about 1690. The corresponding values of $(L_e/d)$ for a circular section are 690 and 980 respectively. Though this situation may not normally be encountered in practice theoretically it is possible to get linear elastic lateral instability even for circular sections.

## 6. CONCLUSIONS

The paper presents a unified solution for various boundary conditions for the problem of coupled flexural–torsional instability of beam-columns of warpless section subjected to axial loads and end moments. By suitable transformations (i) the load interaction equation is obtained independent of the boundary condition in a form similar to that for simply supported ends, (ii) the location of centre of rotation of the cross-section is obtained as a single equation and (iii) the characteristic equations for eigen coefficient $\alpha$ are obtained independent of the loads which are the same as those obtained for the simple case of Euler buckling. The results show that for all practical purposes the results for an infinitely slender beam can give sufficiently accurate results for all slenderness and the correction for finite slenderness is only marginal. The results also show that elastic lateral instability is possible even in the presence of tensile axial loads if the beam is sufficiently slender.

*Acknowledgements*—The work presented in this paper forms a part of a project sponsored by the Aeronautics Research and Development Board, Directorate of Aeronautics, Ministry of Defence, Government of India. The financial support received is gratefully acknowledged.

## REFERENCES

1. S. Timoshenko, *Theory of Elastic Stability*, p. 279. McGraw Hill, New York (1963).
2. B. Johnston, Lateral buckling of $I$-section column with eccentric loads in the plane of web. *J. Appl. Mech.* **8**, A-176 (1941).
3. J. N. Goodier, Torsional and flexural buckling of bars of thin-walled open section under compressive and bending loads. *J. Appl. Mech.* **9**, A-103 (1942).
4. M. G. Salvadori, Lateral buckling of $I$-beams. *Trans. ASCE* **120**, 1165 (1955).
5. J. W. Clark, Lateral buckling of beams. *Proc. ASCE, J. Structural Div.* **86** (ST-7), 175 (1960).
6. A. Chajes, Torsional–flexural buckling of thin-walled members. *Proc. ASCE, J. Structural Div.* **91** (ST-4), 103 (1965).
7. T. Tarnai, Variational methods for analysis of lateral buckling of beams hung at both ends. *Int. J. Mech. Sci.* **21**, 6, 329 (1979).
8. A. Joshi and S. Suryanarayan, The effect of static axial loads and end moment on the vibration and stability of narrow rectangular beams. Department Tech. Rep. AETR 81121, Dec. 1981, Dept. of Aero. Engng. I.I.T. Bombay (Also presented at the 26th Congress of the Indian Society of Theoretical and Applied Mechanics held at Coimbatore, India from 28–31 Dec. 1981).